Supplemental Information for

Mapping sites of carboxymethyllysine modification on proteins reveals its consequences for proteostasis and cell proliferation

Simone Di Sanzo, Katrin Spengler, Anja Leheis, Joanna M. Kirkpatrick, Theresa L. Rändler, Tim Baldensperger, Luca Parca, Christian Marx, Zhao-Qi Wang, Marcus A. Glomb, Alessandro Ori and Regine Heller

Correspondence to: alessandro.ori@leibniz-fli.de or regine.heller@med.uni-jena.de

This PDF file includes:

Figures S1 to S6

The following supplemental tables are provided as separate Excel files:

Table S1: List of CML sites identified in MEF and HUVEC. Related to Figure 1 and S1.

Table S2: List of CML sites identified in mouse organs and proteome changes induced by aging. Related to Figure 2 and S2.

Table S3: Proteome changes induced in MEF by glyoxal treatment. Related to Figure 3 and S3.

Table S4: Proteome changes induced in HUVEC by glyoxal treatment. Related to Figure 4.

Table S5: List of cell cycle-related proteins affected in HUVEC by glyoxal or directly modified by CML. Related to Figure 5.

Supplemental Figures

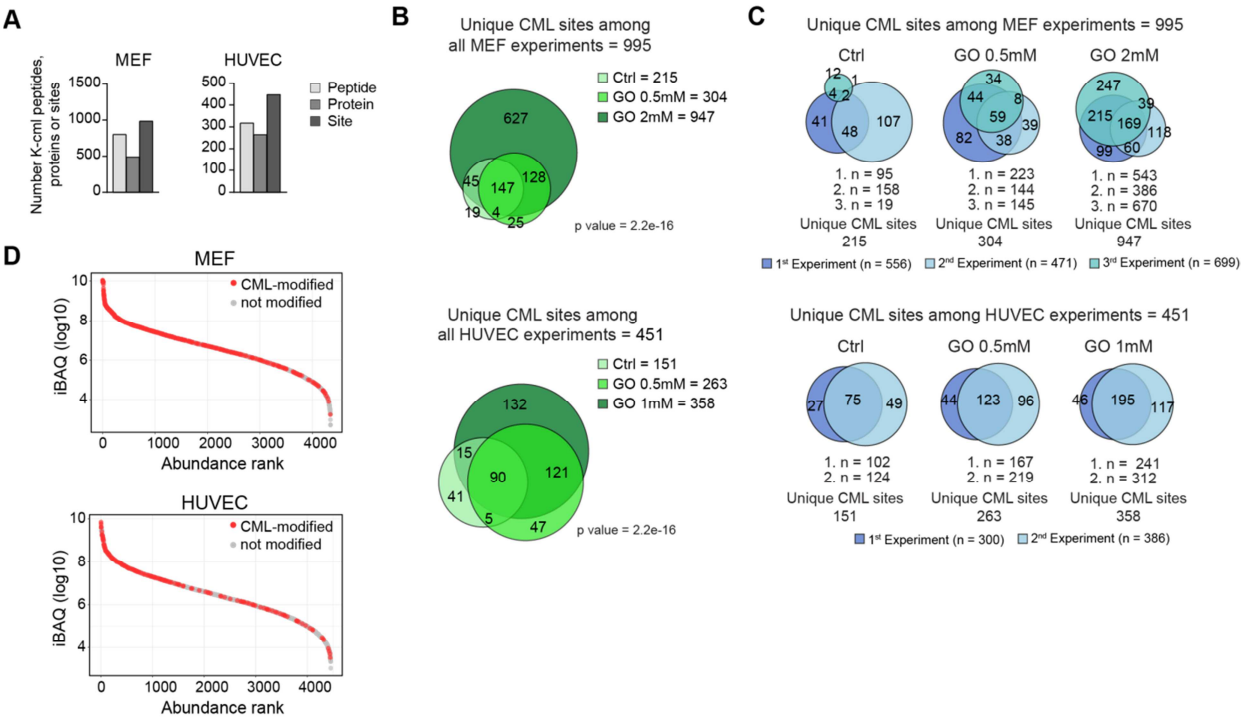

Figure S1.

A. Statistics of CML sites identified in MEF and HUVEC treated with glyoxal. Data from different treatments and biological replicates were combined. **B.** Overlap between CML sites identified under different experimental conditions. **C.** Reproducibility of CML site identification across independent experiments. In B and C, only highly confident sites were considered and the overlap between experiment was tested using Fisher's exact test. **D.** Rank plot showing the abundance distribution of proteins identified as targets of CML. Related to Figure 1 and Table S1.

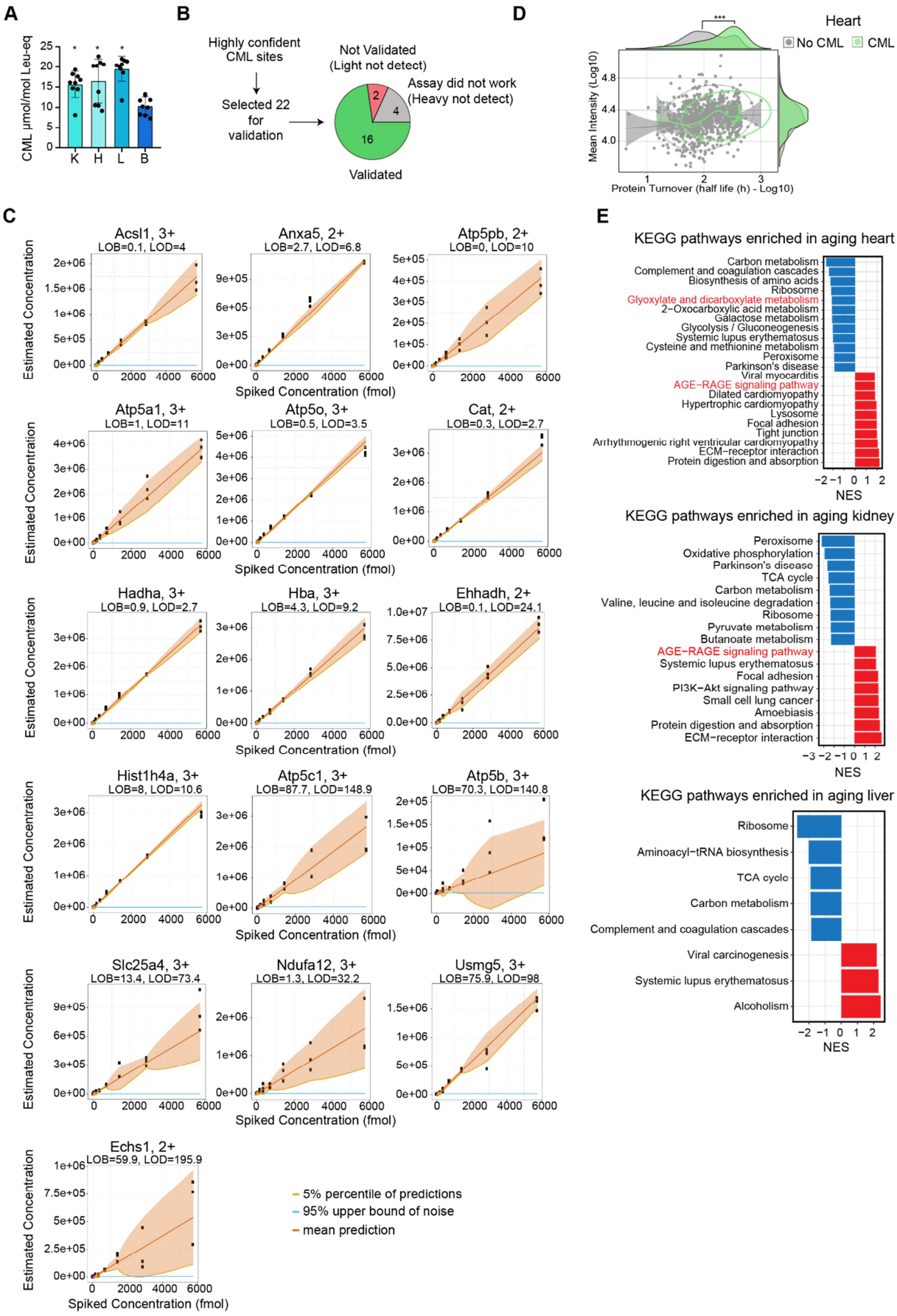
A
CML µmol/mol Leu-eq
K H L B
B
Highly confident CML sites
Selected 22 for validation
Not Validated (Light not detect)
Assay did not work (Heavy not detect)
Validated
2
4
16
D
Heart
No CML
CML
***
Mean Intensity (Log10)
Protein Turnover (half life (h) - Log10)
C
Acsl1, 3+ LOB=0.1, LOD=4
Anxa5, 2+ LOB=2.7, LOD=6.8
Atp5pb, 2+ LOB=0, LOD=10
Atp5a1, 3+ LOB=1, LOD=11
Atp5o, 3+ LOB=0.5, LOD=3.5
Cat, 2+ LOB=0.3, LOD=2.7
Hadha, 3+ LOB=0.9, LOD=2.7
Hba, 3+ LOB=4.3, LOD=9.2
Ehhadh, 2+ LOB=0.1, LOD=24.1
Hist1h4a, 3+ LOB=8, LOD=10.6
Atp5c1, 3+ LOB=87.7, LOD=148.9
Atp5b, 3+ LOB=70.3, LOD=140.8
Slc25a4, 3+ LOB=13.4, LOD=73.4
Ndufa12, 3+ LOB=1.3, LOD=32.2
Usmg5, 3+ LOB=75.9, LOD=98
Echs1, 2+ LOB=59.9, LOD=195.9
Estimated Concentration
Spiked Concentration (fmol)
5% percentile of predictions
95% upper bound of noise
mean prediction
E
KEGG pathways enriched in aging heart
Carbon metabolism
Complement and coagulation cascades
Biosynthesis of amino acids
Ribosome
Glyoxylate and dicarboxylate metabolism
2-Oxocarboxylic acid metabolism
Galactose metabolism
Glycolysis / Gluconeogenesis
Systemic lupus erythematosus
Cysteine and methionine metabolism
Peroxisome
Parkinson's disease
Viral myocarditis
AGE-RAGE signaling pathway
Dilated cardiomyopathy
Hypertrophic cardiomyopathy
Lysosome
Focal adhesion
Tight junction
Arrhythmogenic right ventricular cardiomyopathy
ECM-receptor interaction
Protein digestion and absorption
NES
KEGG pathways enriched in aging kidney
Peroxisome
Oxidative phosphorylation
Parkinson's disease
TCA cycle
Carbon metabolism
Valine, leucine and isoleucine degradation
Ribosome
Pyruvate metabolism
Butanoate metabolism
AGE-RAGE signaling pathway
Systemic lupus erythematosus
Focal adhesion
PI3K-Akt signaling pathway
Small cell lung cancer
Amoebiasis
Protein digestion and absorption
ECM-receptor interaction
NES
KEGG pathways enriched in aging liver
Ribosome
Aminoacyl-tRNA biosynthesis
TCA cycle
Carbon metabolism
Complement and coagulation cascades
Viral carcinogenesis
Systemic lupus erythematosus
Alcoholism
NES

Figure S2.

A. Quantification of total CML levels in mouse organs. K: kidney, H: heart, L: liver, B: brain. n=9. * p<0.05 vs. brain, ordinary one-way ANOVA. **B.** Validation of identified CML sites using parallel reaction monitoring (PRM) and heavy labelled spiked-in reference peptides. **C.** Limit of detection (LOD) and limit of blank (LOB) for PRM assays targeting selected CML sites. Dilution series of synthetic heavy peptides were used for LOB and LOD estimation (see Methods for details). **D.** Protein turnover of CML-modified proteins grouped according to their subcellular localization, as defined by Gene Ontology annotation. Turnover data were taken from (Fornasiero et al., 2018). C: cytoplasm; ER: endoplasmic reticulum; GA: Golgi apparatus; M: mitochondria; N: nucleus. Scatterplot comparing protein abundance (average protein intensity) and protein turnover (half life) of CML-modified proteins. Density plot shows the distribution of each dataset. n=5. *** p<0.001, Wilcoxon Rank Sum test with continuity correction. **E.** KEGG pathway Gene Set Enrichment Analysis (GSEA) in aging tissues performed using WebGestalt. Normalized enrichment score (NES) indicates pathways enriched among proteins that increase (red) or decrease (blue) with aging (FDR<0.05). All the proteins quantified in each experiment were ranked according to their log2 fold change and used as input for GSEA. Related to Figure 2 and Table S2.

A

ID	Gene	Type	Protein name	Where (CML site)
Q9R1P1	PSMB3	26S Proteasome	Proteasome subunit beta type-3	Liver (15)
Q9R1P4	PSMA1	26S Proteasome	Proteasome subunit alpha type-1	MEF (30)
Q8C7R4	UBA6	E1 ligase	Ubiquitin-like modifier-activating enzyme 6	MEF (519)
Q9Z1F9	UBA2	E1 ligase	SUMO-activating enzyme subunit 2	MEF (271), HUVEC (271)
Q6ZPJ3	UBE2O	E2 ligase	E2/E3 hybrid ubiquitin-protein ligase UBE2O	Kidney (885, 888), MEF (368, 379, 380, 382, 360)
Q61187	TSG101	E2 ligase	Tumor susceptibility gene 101 protein	Kidney (9, 10)
P68037	UBE2L3	E2 ligase	Ubiquitin-conjugating enzyme E2 L3	MEF (73)
Q69ZR2	HECTD1	E3 ligase	E3 ubiquitin-protein ligase HECTD1	Kidney (2285, 2290)
Q7TMY8	HUWE1	E3 ligase	E3 ubiquitin-protein ligase HUWE1	MEF (4137, 4142, 3257, 3274), HUVEC (4134, 4139)
P46935	NEDD4	E3 ligase	E3 ubiquitin-protein ligase NEDD4	MEF (186, 429, 484)
Q8BFU3	RNF214	E3 ligase	RING finger protein 214	MEF (136, 142)
P58283	RNF216	E3 ligase	E3 ubiquitin-protein ligase RNF216	MEF (629)
Q8K2Y0	RNF219	E3 ligase	RING finger protein 219	MEF (498, 505)
Q62318	TRIM28	E3 ligase	Transcription intermediary factor 1-beta	MEF (770, 774, 779), HUVEC (366, 304)
Q6WKZ8	UBR2	E3 ligase	E3 ubiquitin-protein ligase UBR2	MEF (1496)
A2AN08	UBR4	E3 ligase	E3 ubiquitin-protein ligase UBR4	MEF (1929), HUVEC (1060, 1931, 1141, 1150)
Q0P5W1	VPS8	E3 ligase	Vacuolar protein sorting-associated protein 8 homolog	MEF (1313, 1316)
Q80YR4	ZNF598	E3 ligase	Zinc finger protein 598	MEF (94)
Q9Y4D8	HECTD4	E3 ligase	Probable E3 ubiquitin-protein ligase HECTD4	HUVEC (2326, 2331)
P29590	PML	E3 ligase	Protein PML	HUVEC (487, 490)
P0CG49	UBB	Ubiquitin	Polyubiquitin-B	Heart (11), HUVEC (11, 63), MEF (6, 11, 63)
P0CG50	UBC	Ubiquitin	Polyubiquitin-C	Heart (11), HUVEC (11, 63), MEF (6, 11, 63)
P62983	RPS27A	Ubiquitin	Ubiquitin-40S ribosomal protein S27a	Heart (11), HUVEC (11, 63), MEF (6, 11, 63)
P62984	UBA52	Ubiquitin	Ubiquitin-60S ribosomal protein L40	Heart (11), HUVEC (11, 63), MEF (6, 11, 63)
Q99LD4	GPS1	UPS associated	COP9 signalosome complex subunit 1	MEF (204)
P56399	USP5	UPS associated	Ubiquitin carboxyl-terminal hydrolase 5	MEF (288, 291), HUVEC (288, 291)
P35125	USP6	UPS associated	Ubiquitin carboxyl-terminal hydrolase 6	HUVEC (313)

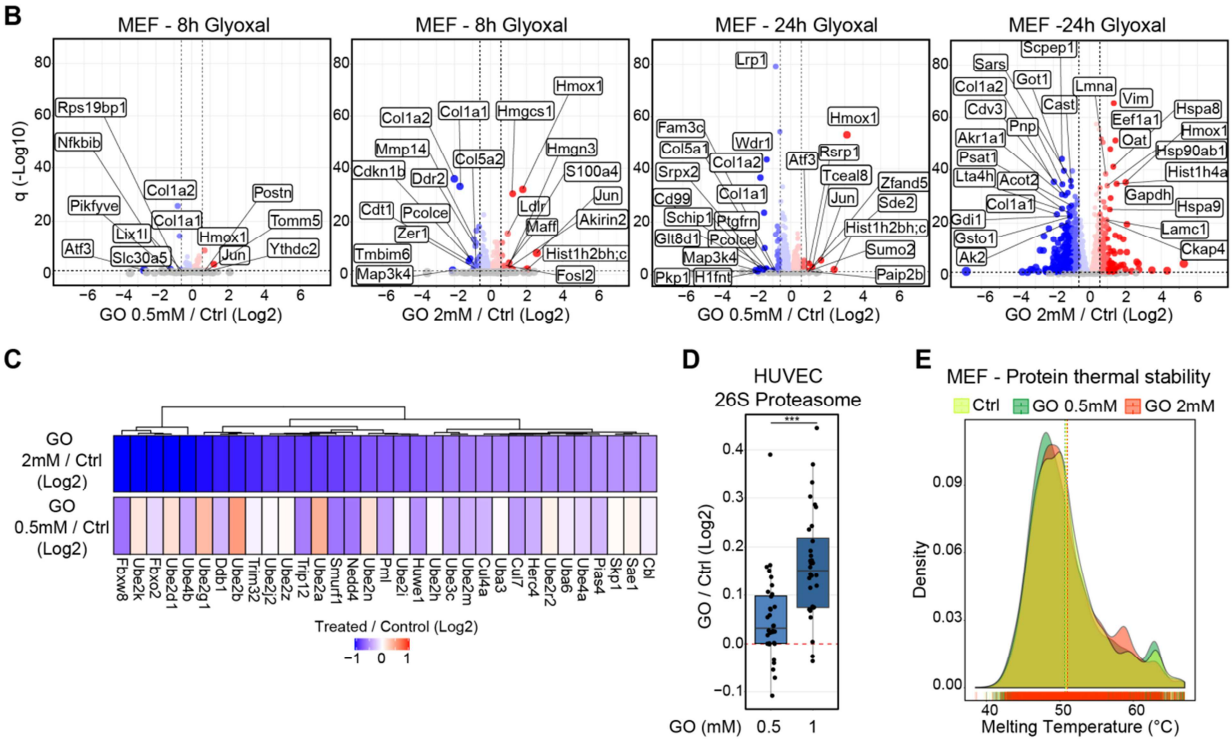

Figure S3.

A. Table of CML sites identified on proteins related to the ubiquitin proteasome system. **B.** Protein abundance changes induced in MEF treated with glyoxal (GO). Volcano plots depict proteins that significantly increase (red) or decrease (blue) abundance upon GO treatment. Proteins not affected are shown in gray. Horizontal dashed line indicates a significance cut-off of q<0.05 and vertical dashed lines an absolute fold change (log2)>0.58. **C.** Heatmap representing the protein abundance of protein involved in the ubiquitin-mediated proteolysis (Fig. 3D in red) induced in MEF by 0.5 mM and 2 mM GO after 24 h of treatment. **D.** Boxplot of fold changes for members of the 26S proteasome in HUVEC cells treated with GO for 48 h compared to control (Ctrl). n=4. *** p<0.001, Wilcoxon Rank Sum test with continuity correction. **E.** Effect of GO on protein thermal stability in MEF treated for 24 h. Melting temperatures for 4367 (Ctrl), 4174 (GO 0.5 mM) and 4646 (GO 2 mM) protein groups were estimated using thermal proteome profiling (see Methods for details). Related to Figure 3 and Table S3.

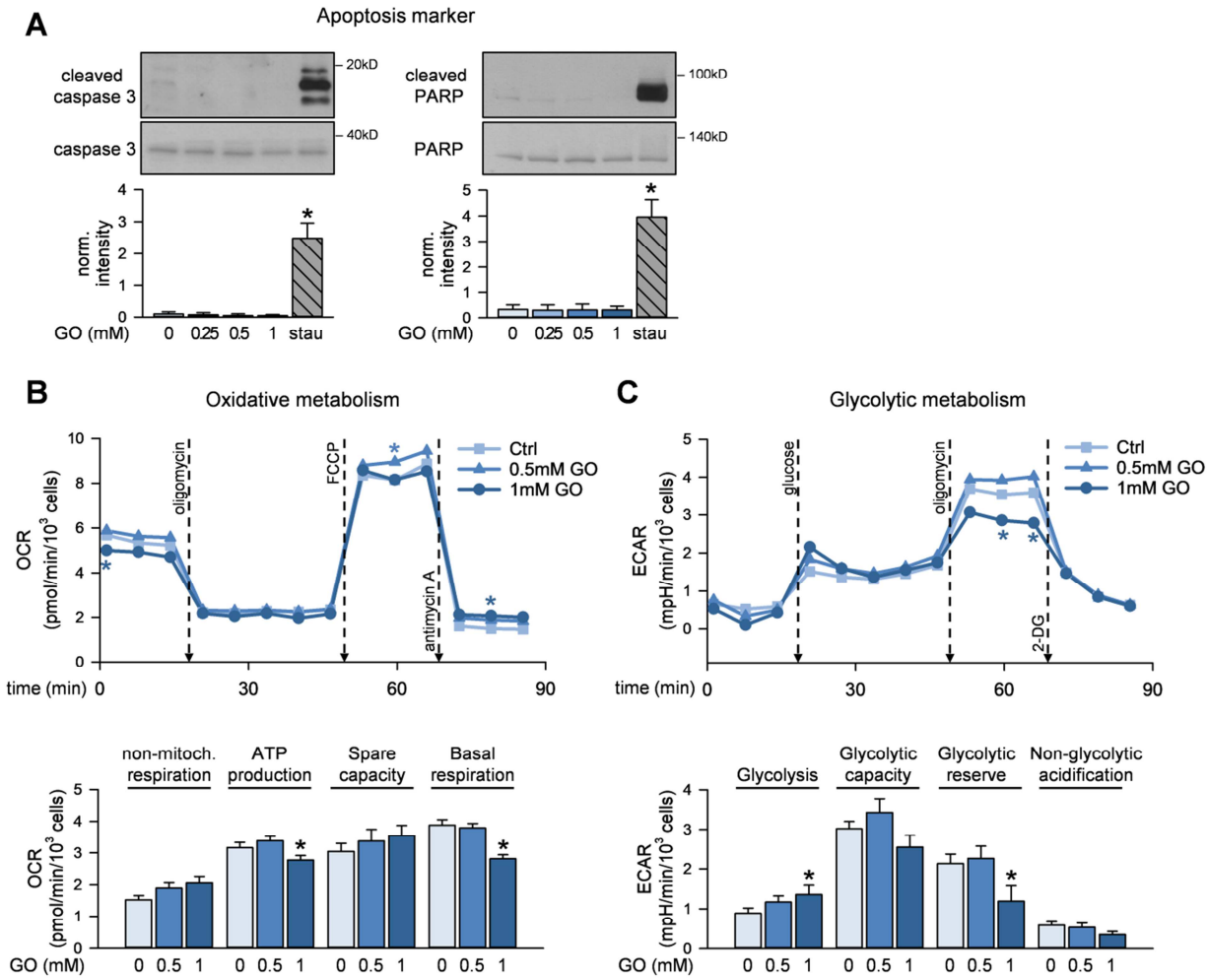

Figure S4.

A. HUVEC were treated with the indicated concentrations of glyoxal (GO) for 48 h. The positive control was treated with 1 µM staurosporin (stau) for 2 h. Immunofluorescence staining of γH2AX (S139) and DAPI staining were performed. Cell lysates were subjected to immunoblot analysis. n=4, * p<0.05 vs. control. **B.** Mito stress test: After GO treatment (48 h) oxygen consumption rates (OCR) were measured via the Seahorse technology at baseline and after addition of pharmacological agents (oligomycin - inhibitor of mitochondrial electron transport chain (ETC) complex V, the ATP synthase; carbonyl cyanide-4-(trifluoromethoxy)phenylhydrazone (FCCP) - mitochondrial uncoupling agent; antimycin A - inhibitor of ETC complex III). Non-mitochondrial respiration, ATP production, spare capacity and basal respiration were calculated from OCR values. **C:** Glycolysis stress test: After GO treatment (48 h) extracellular acidification rates (ECAR) were measured via the Seahorse technology at baseline and after addition of glucose, oligomycin and 2-deoxy-D-glucose, an inhibitor of glycolysis. Glycolytic activity, capacity and reserve, and non-glycolytic acidification were calculated from the measured ECAR data. Upper panels show the time-dependent measurement of OCR and ECAR. Lower panels display the calculated metabolic parameters. n=6. * p<0.05 vs. control. Statistical significance was analyzed using one-way repeated measurement ANOVA corrected using Holm-Šidák method. Related to Figure 4.

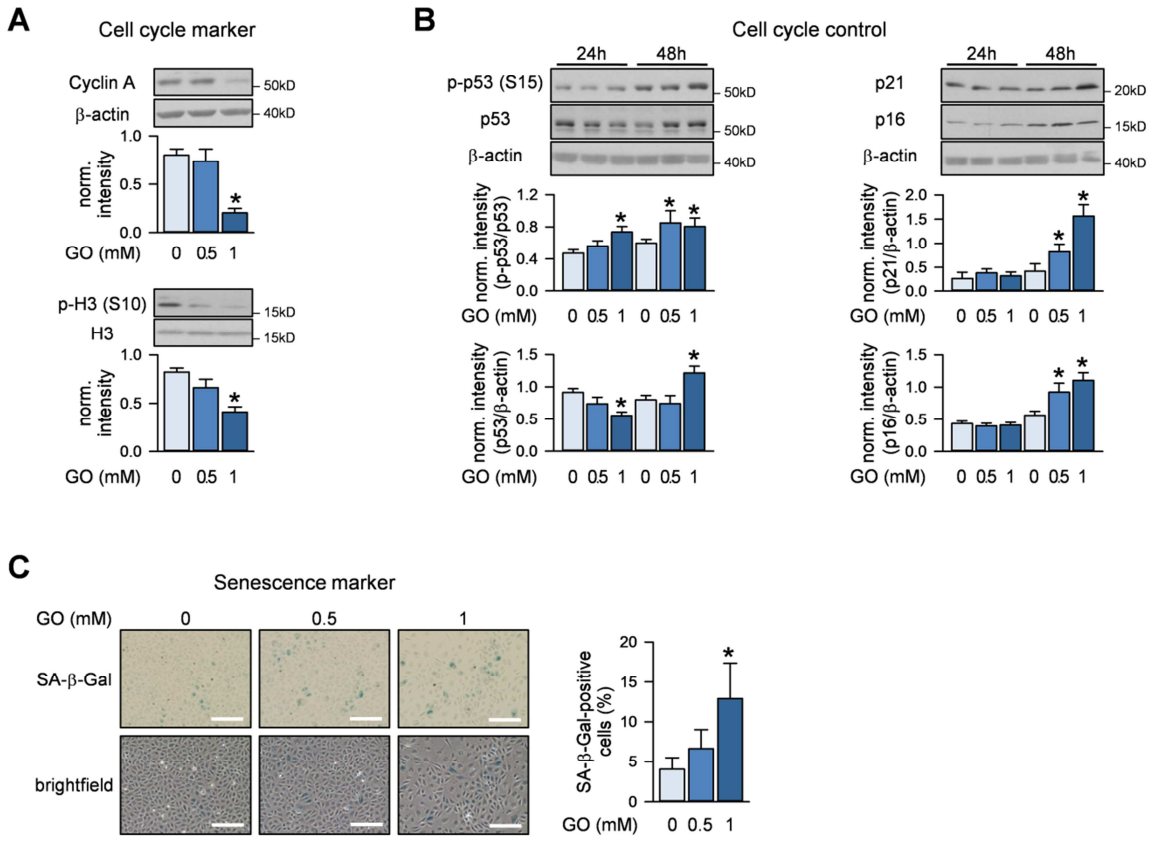

Figure S5.

A-C.: HUVEC were treated with GO at the indicated concentrations for 24 h (**A,B**) or 48 h (**B,C**). **A-B**. Cell lysates were subjected to immunoblot analysis of cell cycle regulators. n=6 (**A**), n=5 (**B**), * p<0.05 vs. respective control. **C**. Senescence-associated β-galactosidase (SA-β-Gal) was stained. Representative pictures and quantification of SA-β-Gal-positive cells are shown. n=5, * p<0.05 vs. control. Statistical significance was analyzed using one-way repeated measurement ANOVA corrected using Holm-Šidák method. Related to Figure 5.

ID	Gene	Protein name	Where (CML site)
P05213	Tubulin alpha-1B chain	TUBA1B	MEF (336, 338, 326, 394, 401, 163, 164, 96, 352, 370, 60), HUVEC (394, 401, 336, 338, 163, 164)
P68369	Tubulin alpha-1A chain	TUBA1A	MEF (336, 338, 326, 394, 401, 163, 164, 96, 60, 352, 370), HUVEC (394, 401, 326, 336, 338, 163, 164)
P05214	Tubulin alpha-3 chain	TUBA3A	MEF (336, 338, 326, 394, 401, 163, 164, 96, 60, 352, 370)
P68373	Tubulin alpha-1C chain	TUBA1C	MEF (336, 338, 326, 394, 401, 163, 164, 96, 60, 352, 370), HUVEC (394, 401, 326, 336, 338, 163, 164)
P68368	Tubulin alpha-4A chain	TUBA4A	MEF (394, 401, 163, 352, 370), HUVEC (394, 401, 163, 164)
Q9JJZ2	Tubulin alpha-8 chain	TUBA8	MEF (394, 401, 96, 352, 370)
P68372	Tubulin beta-4B chain	TUBB4B	MEF (58, 379, 324, 336, 103, 216), Kidney (324)
P99024	Tubulin beta-5 chain	TUBB5	MEF (362, 379, 58, 324, 336, 103, 216), Kidney (324)
Q922F4	Tubulin beta-6 chain	TUBB6	MEF (57, 58)
Q3UX10	Tubulin alpha chain-like 3	TUBAL3	MEF (401), HUVEC (401, 408)
Q7TMM9	Tubulin beta-2A chain	TUBB2A	MEF (379, 324, 336, 103, 216), HUVEC (324, 103, 379), Kidney (324)
Q9CWF2	Tubulin beta-2B chain	TUBB2B	MEF (379, 324, 336, 103, 216), HUVEC (324, 103, 379), Kidney (324)
Q9D6F9	Tubulin beta-4A chain	TUBB4A	MEF (103, 216), HUVEC (58, 324, 103)
Q13748	Tubulin alpha-3C/D chain	TUBA3C	HUVEC (394, 401, 326, 336, 338, 163, 164)
P07437	Tubulin beta chain	TUBB	HUVEC (58, 379, 324, 103)
Q6PEY2	Tubulin alpha-3E chain	TUBA3E	HUVEC (326, 336, 338)
Q13509	Tubulin beta-3 chain	TUBB3	HUVEC (58)
P04350	Tubulin beta-4A chain	TUBB4A	HUVEC (103)

Figure S6.
Table of CML sites identified on tubulins. Related to Figure 6.